Corrosion-Induced Concrete Cracking for Uncoated and Galvanized Reinforcing Bars

by Matthew O'Reilly, Omid Farshadfar, David Darwin, JoAnn Browning, and Carl E. Locke Jr.

Corrosion-related cracking in reinforced concrete is caused by expansive corrosion products and the resulting tensile stresses. While the amount of corrosion to cause cracking has been studied for uncoated conventional reinforcement, significantly less is known about the corrosion loss at cracking for galvanized reinforcement. Conventional and galvanized bars were cast in chloride-contaminated concrete. Clear cover to the bar ranged from 0.5 to 2 in. (12.7 to 51 mm). Specimens were tested both with and without the use of impressed current to drive corrosion. It was found that galvanized reinforcement requires greater corrosion losses to crack concrete than conventional steel reinforcement. Visual observations at autopsy suggest that the cracking of the concrete specimens containing galvanized reinforcement was not due to zinc corrosion products, but rather to corrosion products from intermetallic iron-zinc layers or from the underlying steel. Further study is needed to determine the exact nature of these corrosion products. Tests using impressed current may be used to establish the corrosion loss required to cause cracking.

Keywords: chlorides; corrosion; cracking; galvanized reinforcement; steel reinforcement; zinc.

INTRODUCTION

The corrosion of reinforcing steel plays a major role in determining the life expectancy of many reinforced concrete structures. The time to repair of a structure due to corrosion-related damage depends on the time it takes for corrosion of the reinforcement to initiate and the time for corrosion products to create tensile stresses sufficient to crack the concrete cover. The latter is a function of the corrosion rate of the reinforcement and the corrosion loss needed to crack the concrete cover.

The corrosion products of steel create tensile forces in the surrounding concrete, eventually resulting in cracking and spalling of the concrete cover. Several studies have used impressed current, chloride-contaminated concrete, or both, to establish a relationship, often in the form of an expression connecting the corrosion loss to cause cracking with member geometry and the thickness of the concrete cover for uncoated conventional reinforcement (Rasheeduzzafar et al. 1992a; Alonso et al. 1998; El Maaddawy and Soudki 2003; Torres-Acosta and Sagues 2004; Xia and Jin 2014; Abouhussien and Hassan 2016). The corrosion of galvanized reinforcement, however, initially involves the loss of zinc, not iron, preventing the application of these results to galvanized reinforcement.

The galvanizing process results in the formation of an outer layer of pure zinc that is underlain by several layers of intermetallic iron-zinc alloys. The outer zinc layer on galvanized reinforcement helps protect the steel from corrosion by acting as a barrier to moisture and oxygen, raising the critical chloride corrosion threshold (Darwin et al. 2009) and serving as a sacrificial anode. The underlying zinc-iron alloy layers provide no corrosion protection (Andrade and Macias 1988). Only limited research has been performed on the amount of corrosion loss required to crack concrete for galvanized reinforcement, and there is some uncertainty over the form the zinc corrosion products take. Sergi et al. (1985) found that the initial corrosion product of zinc is often zinc oxide (ZnO). The volume of zinc oxide is only 1.5 times that of solid zinc (Hime and Machin 1993), and while many oxidized forms of iron exist, the volume of ferric oxide has been estimated at approximately three times that of solid steel (Suda et al. 1993). In concrete, zinc oxide is converted to calcium hydroxyzincate. Belaïd et al. (2001) observed the formation of a more porous interfacial transition zone adjacent to the zinc-cement paste interface than forms at the surface of steel reinforcement into which the calcium hydroxyzincate later diffuses.

The previous observations indicate that the corrosion loss required to crack concrete containing galvanized reinforcement should be greater than the corrosion loss required to crack concrete with conventional reinforcement. Under certain conditions, however, zinc can also form zinc hydroxychloride II ($Zn_5(OH)_8Cl_2 \cdot H_2O$) (Sergi et al. 1985), which has 3.6 times the volume of solid zinc (Hime and Machin 1993). The formation of zinc hydroxychloride II will result in corrosion losses for galvanized reinforcement at the onset of cracking similar to those observed for conventional reinforcement. Tittarelli et al. (2000) found that galvanized plates in cracked concrete and exposed to cyclic exposure to a 10% NaCl solution exhibited corrosion rates similar to that of uncoated steel. Rasheeduzzafar et al. (1992b) studied conventional and galvanized reinforcement cast in concrete with chloride contents at casting ranging from 4 to 32 lb/yd³ (2.4 to 19.2 kg/m³). Rasheeduzzafar et al. found that specimens containing galvanized reinforcement took longer to crack concrete than specimens containing conventional reinforcement; however, the corrosion loss at crack initiation was not determined.

Numerous models have been developed in recent years that predict the propagation of damage in reinforced

concrete structures containing conventional reinforcement (Torres-Acosta and Sagues 2004; Zhao et al. 2011; Nossoni and Harichandran 2014). However, to date, no such model exists for galvanized reinforcement. A probabilistic service-life model examining conventional and galvanized reinforcement developed by Williamson et al. (2009) predicted the service life for bridge decks containing galvanized reinforcement to be approximately twice that of decks containing conventional reinforcement. This model, however, was based on field observations predicting a time to cracking of 6 years for conventional reinforcement (Williamson 2007) and a conceptual model of galvanized reinforcement that predicted a time to cracking of 20 years (Yeomans 1994), and did not feature a direct comparison of corrosion loss at cracking. Previous research analyzing the corrosion products of galvanized reinforcement leaves some question as to whether the corrosion loss to crack concrete for galvanized reinforcement would be greater or less than that of conventional reinforcement.

To answer this question, the research presented in this paper examines the corrosion losses required to crack concrete for conventional and galvanized reinforcement. Specimens are tested with varying values of concrete cover over the reinforcement to establish a relationship between corrosion loss and cracking for conventional and galvanized reinforcement. Specimens with 1 in. (25 mm) cover to the bar were evaluated both with and without an impressed current to determine if the application of impressed current results in corrosion and cracking behavior that is representative of reinforcing steel corrosion cells that are not forced.

RESEARCH SIGNIFICANCE

Extending the service life of reinforced concrete structures may be achieved by increasing the time to initiation of corrosion or by increasing the time between initiation and spalling of the concrete. While this is often achieved by using a material with a lower corrosion rate after initiation, a material with a less expansive corrosion product would also exhibit an increased service life. Quantifying the extent, if any, to which galvanized reinforcement increases the time to cracking will allow designers to more realistically estimate service-life costs when using galvanized reinforcement, resulting in cost savings and more durable structures.

EXPERIMENTAL PROCEDURES

Specimens were tested both with and without impressed current driving the corrosion rate. Schematics of these specimens are shown in Fig. 1(a) and 1(b), respectively. The design was similar for specimens with and without impressed current. The specimens were 6 in. (152 mm) wide by 12 in. (305 mm) long, with the height of the specimen adjusted to provide different values of clear concrete cover over the reinforcement. A concrete dam, cast integrally with the specimen, allowed for the ponding of water or salt solution. The reinforcement consisted of No. 5 (No. 16) deformed bars. The top reinforcing bar consisted of conventional or galvanized steel; the bottom bars were pickled 2205 duplex stainless steel to prevent corrosion of these bars. Full details on the test procedures are provided by O'Reilly et al. (2011), Darwin et al. (2011), and Farshadfar et al. (2017).
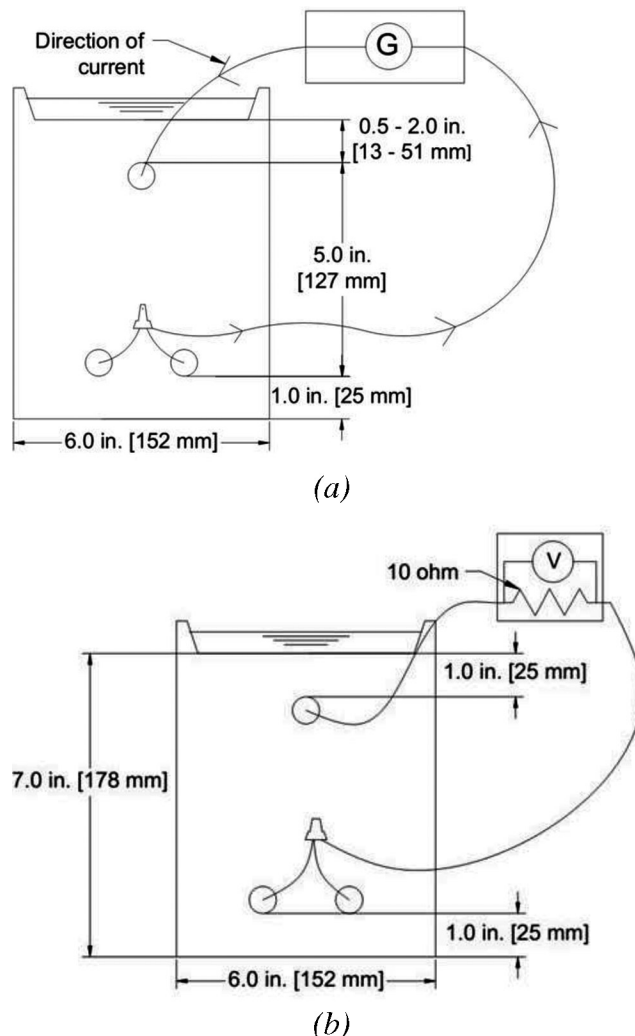

Fig. 1—Cracking specimen: (a) with impressed current; and (b) without impressed current.

Specimens with impressed current

The specimens with impressed current were used to gain information regarding crack initiation and propagation in a relatively short time. For these specimens, the top and bottom bars were connected across a 30 V power supply to provide an impressed current. The current to each specimen was measured daily. Assuming uniform corrosion on the top bar, the corrosion current density i (traditionally expressed in $\mu A/cm^2$) is found by dividing the measured current by the surface area of the test bar. Current density is used to determine corrosion rate R (in mils/yr or $\mu m/yr$) using Faraday's Law (Eq. (1))

$$R = k\frac{ia}{nF\rho} \tag{1}$$

where k is conversion factor = 12,416 A·mil·s/(μA·cm·y), 315,360 A·μm·s/(μA·cm·y); a is atomic weight of the corroding metal, g/mol; n is number of electrons lost per atom of metal oxidized; F is Faraday's constant = 96,485 Coulombs/equivalent; and ρ is density of metal, g/cm^3.

For iron, a = 55.85 g/mol, n = 2, ρ = 7.87 g/cm^3, and Eq. (1) simplifies to $R = 0.457i$ in mils/y or $11.6i$ in $\mu m/y$. For zinc, a = 65.38 g/mol, n = 2, ρ = 7.13 g/cm^3, and Eq. (1)

Table 1—Concrete mixture proportions

Cement[*], lb/yd³ (kg/m³)	Water, lb/yd³ (kg/m³)	Fine aggregate[†], lb/yd³ (kg/m³)	Coarse aggregate[‡], lb/yd³ (kg/m³)	NaCl[§], lb/yd³ (kg/m³)	AEA[||], oz/yd³ (L/m³)
598 (356)	269 (160)	1435 (854)	1484 (883)	19.8 (11.7)	68.9 (2.66)

[*]Type I/II portland cement.
[†]Bulk specific gravity (SSD) = 2.62, absorption 0.8%, fineness modulus 2.51.
[‡]Crushed limestone. Nominal maximum size 0.75 in. (19 mm), bulk specific gravity (SSD) = 2.58, absorption 2.3%, unit weight 95.9 lb/ft³ (1536 kg/m³).
[§]2% by weight of cement.
[||]Air-entraining agent, neutralized rosin.

simplifies to $R = 0.591i$ in mils/y or $15.0i$ in μm/y. Corrosion loss (representing the average depth of material lost) is obtained by integrating the corrosion rate over time.

During the test, the specimens were ponded with deionized water. The current density was measured daily for each specimen; the range was 67 to 148 μA/cm², and the average was close to 100 μA/cm². Specimens were also visually monitored daily for staining and cracking. The corrosion losses corresponding to staining, crack initiation, and propagation of the crack to the full specimen length were recorded. In addition, once a crack formed, the crack width was measured and tracked using a crack comparator. At the completion of testing, specimens were autopsied, the top bars were photographed, and a visual estimation of the corroded surface area was performed by overlaying a clear grid on the surface of the bar.

Specimens without impressed current

Specimens with no external source driving corrosion—that is, without impressed current—were also evaluated as a means of validating the results obtained from the impressed current specimens. Due to the extended nature of this test, testing was terminated after crack initiation. For these specimens, the corrosion rate was measured using linear polarization resistance (LPR). This technique induces small changes in potential on the corroding bar, measuring the current associated with each change potential to determine the corrosion rate. A scan range of –20 mV to +20 mV with respect to the equilibrium potential was used with a scan rate of 0.125 mV/s; polarization resistance was established over the range –10 mV to +10 mV. LPR was used for these specimens because, without an external current forcing corrosion, significant amounts of corrosion would occur between anodes and cathodes located on the top bar (microcell corrosion) that would not be detected by measuring the current flow between the top and bottom bars (as was done for impressed current specimens). LPR readings were taken monthly. Corrosion potential readings were taken on a weekly basis to verify that continuous active corrosion was occurring.

Specimens without impressed current were subjected to alternating cycles of ponding and drying with a 15% NaCl solution. During the first cycle, specimens were ponded with the solution for 4 days at 72°F (22°C), followed by 3 days of drying under heat tents at 100°F (38°C). This pattern was repeated for 12 weeks, after which the specimens were ponded for 12 weeks at 72°F (22°C). The two exposure regimes were repeated until specimens were removed from testing. Upon completion of testing, specimens were autopsied, photographed, and the corroded surface area of the top

Table 2—Number of specimens in test program

Reinforcement	Test program	Cover		
		0.5 in. (12.7 mm)	1.0 in. (25.4 mm)	2.0 in. (51 mm)
Conventional (Conv.)	Impressed current	4	4	4
	No impressed current	—	6	—
Galvanized (Zn)	Impressed current	4	6[*]	4
	No impressed current	—	6	—

[*]Two specimens removed from testing at crack initiation.

bar visually estimated in the same manner as used for the impressed current specimens.

Materials and test program

The concrete mixture proportions used for the test specimens are listed in Table 1. The concrete had a water-cement ratio (w/c) of 0.45, representative of concrete used in low-cracking bridge decks (Darwin et al. 2010). Compressive strengths at 28 days ranged between 4090 and 4490 psi (28.2 and 31.0 MPa). To destabilize the passive layer of the reinforcement and increase ion conductivity of the concrete, NaCl equivalent to 2% chlorides by weight of cement was dissolved in the mixing water prior to casting.

The conventional bars met the requirements of ASTM A615. The galvanized bars had a nominal zinc coating thickness of 6 mils (0.150 mm) and met the requirements of ASTM A767, except that the bars were not dipped in a chromate bath after coating. The latter is used to passivate the zinc surface and prevent the zinc from reacting with hydroxyl ions in fresh concrete.

The test program, summarized in Table 2, consisted of 38 specimens: 26 with impressed current and 12 without. The top bars in the impressed current specimens had concrete covers of 0.5, 1, and 2 in. (12.7, 25.4, and 51 mm), while the 12 specimens without impressed current had a concrete cover of 1 in. (25.4 mm).

EXPERIMENTAL RESULTS
Specimens with impressed current

The average values of corrosion loss corresponding with staining, initial cracking, and crack widths ranging from 10 to 20 mils (0.25 to 0.50 mm) for conventional and galvanized reinforcement are summarized for the specimens with impressed current in Table 3. Crack initiation could be observed once the cracks reached widths of 2 to 4 mils (0.05

Table 3—Average corrosion losses for conventional and galvanized reinforcement for specimens with impressed current, mils

	Cover					
	0.5 in. (12.7 mm)		1 in. (25.4 mm)		2 in. (51 mm)	
	Conv.	Zn	Conv.	Zn	Conv.	Zn
Staining						
Average	0.265	1.40	0.745	1.66	1.13	3.43
Standard deviation	0.103	0.616	0.376	0.357	0.112	—*
Coefficient of variation	0.390	0.441	0.505	0.215	0.099	—*
Crack initiation						
Average	0.415	1.81	0.883	1.96	1.17	2.44
Standard deviation	0.110	0.671	0.218	0.379	0.183	0.720
Coefficient of variation	0.265	0.371	0.247	0.194	0.156	0.295
10 mil (0.25 mm) crack width						
Average	0.91	2.54	1.53	2.60	1.45	2.70
Standard deviation	0.161	0.954	0.232	0.724	0.198	0.700
Coefficient of variation	0.176	0.376	0.152	0.279	0.136	0.259
13 mil (0.33 mm) crack width						
Average	1.34	3.21	1.81	3.58	1.93	3.22
Standard deviation	0.318	0.917	0.031	1.14	0.328	0.856
Coefficient of variation	0.237	0.285	0.017	0.319	0.170	0.266
16 mil (0.41 mm) crack width						
Average	2.11	3.91	2.12	4.64	2.39	4.16
Standard deviation	0.353	0.977	0.280	0.955	0.385	1.37
Coefficient of variation	0.167	0.250	0.132	0.206	0.161	0.329
20 mil (0.51 mm) crack width						
Average	2.87	4.74	2.98	6.03	2.94	5.22
Standard deviation	0.775	1.29	0.472	1.27	0.585	2.10
Coefficient of variation	0.270	0.272	0.158	0.211	0.199	0.403

*Only one specimen exhibited surface staining.

Note: 1 mil = 25.4 μm = 0.0254 mm.

to 0.10 mm). All specimens initiated cracking in the center third of the specimen. The corrosion losses for individual specimens are presented in Table 4. In all cases, the galvanized reinforcement required significantly greater corrosion losses to crack the concrete than did the conventional reinforcement. For 0.5, 1, and 2 in. (12.7, 25.4, and 51 mm) covers, the conventional reinforcement required average corrosion losses of 0.42, 0.88 and 1.17 mils (11, 22, and 30 μm), respectively, to crack the concrete cover, compared with 1.81, 1.96, and 2.68 mils (46, 50, and 68 μm) for the galvanized reinforcement. Based on Student's t-test, the differences in corrosion loss at first cracking between specimens with conventional and galvanized reinforcement are statistically significant ($p < 0.015$). For conventional reinforcement, increasing the cover from 0.5 to 2 in. (12.7 to 51 mm) nearly tripled the corrosion loss required to crack concrete (an increase of 0.76 mils [19 μm]), while for galvanized reinforcement, the corrosion loss required to crack concrete increased by 48% (an increase of 0.87 mils [22 μm]).

Figure 2 summarizes the average values of corrosion loss corresponding to staining, crack initiation, and various stages of crack growth for the specimens; standard deviations are represented by error bars. The staining of the top surface preceded the formation of a crack in all cases, except for the specimens with galvanized bars with 2 in. (51 mm) cover for which only one out of the four specimens exhibited staining. The figure illustrates that, in addition to the losses corresponding to crack initiation, the losses required to produce a given crack width were considerably higher for galvanized reinforcement than for conventional reinforcement. For example, for conventional reinforcement with 1 in. (25.4 mm) cover, average corrosion losses of 1.53 and 2.98 mils (39 and 76 μm) were required to produce cracks with widths of 10 and 20 mils (0.25 and 0.51 mm), respectively, compared to average losses of 2.60 and 6.03 mils (66 and 153 μm), respectively, for galvanized reinforcement.

Stains on the upper surface of specimens both with conventional and galvanized reinforcement were an orange-brown color, and often green or black (indicating anaerobic corrosion) near the center, as shown in Fig. 3(a) and 3(b) for conventional and galvanized reinforcement, respectively. The green-black stains turned orange with time as the corrosion products continued to oxidize in air. The similarities in corrosion products to the conventional reinforcement suggests that the staining and cracking observed for the galvanized reinforcement may be due to corrosion

Table 4—Corrosion losses at crack initiation for conventional and galvanized reinforcement for specimens with impressed current, mils

Cover, in.	Specimen	Conventional		Galvanized	
		Corrosion loss*	Corrosion loss†	Corrosion loss*	Corrosion loss†
0.5	1	0.352	0.352	2.79	3.98
	2	0.377	0.377	1.59	2.27
	3	0.580	0.580	1.27	1.81
	4	0.354	0.354	1.58	2.26
	Average	0.416	0.416	1.81	2.58
	Std. dev.	0.110	0.110	0.671	0.958
1	1	0.770	0.770	2.12	2.35
	2	1.16	1.159	2.09	2.33
	3	0.659	0.659	2.22	2.47
	4	0.945	0.945	1.39	1.55
	Average	0.883	0.883	1.96	2.17
	Std. dev.	0.218	0.218	0.379	0.421
2	1	1.01	1.006	2.99	3.32
	2	1.20	1.202	2.45	2.72
	3	1.06	1.059	1.42	1.58
	4	1.41	1.414	2.90	3.23
	Average	1.17	1.170	2.44	2.71
	Std. dev.	0.182	0.182	0.720	0.800

*Assuming entire area of bar is undergoing active corrosion.

†Based on percentage of bar surface area exhibiting active corrosion (100% for conventional bars, 90% for galvanized bars with 1 or 2 in. [25.4 or 51 mm] cover, 70% for galvanized bars with 0.5 in. [12.7 mm] cover).

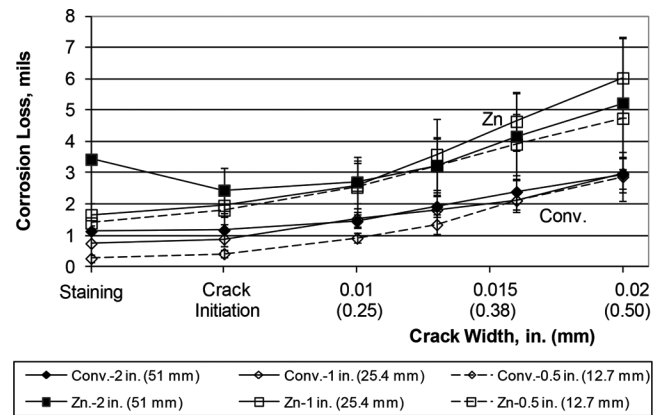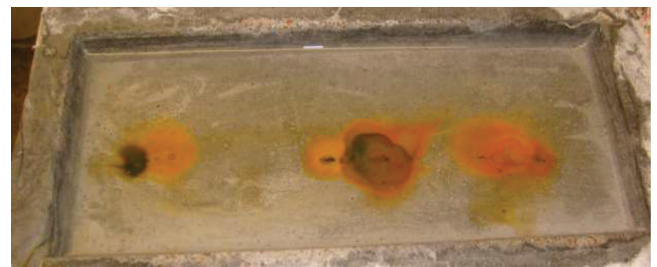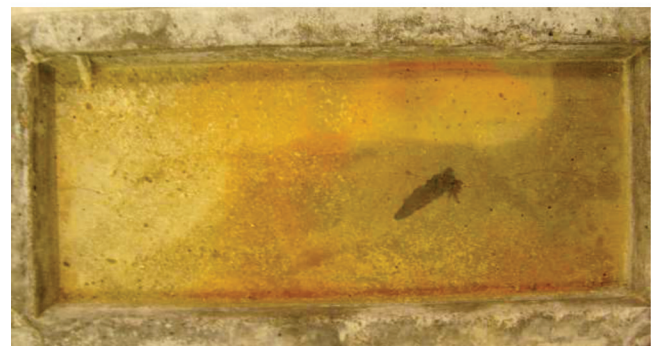Notes: 1 mil = 25.4 μm = 0.0254 mm; 1 in. = 25.4 mm.

Fig. 2—Average corrosion loss at staining, crack initiation, and at stages of crack growth for specimens with impressed current containing conventional (Conv.) and galvanized (Zn) bars. Standard deviation of each value given by error bar. (Note 1 mil = 25.4 μm.)

(a)

(b)

Fig. 3—Concrete surface after crack initiation: (a) conventional reinforcement, impressed current, 1 in. (25.4 mm) cover; and (b) galvanized reinforcement, impressed current, 1 in. (25.4 mm) cover.

of the intermetallic iron-zinc layers or of the underlying steel. Staining increased for specimens with both conventional and galvanized reinforcement as the tests progressed, although, in general, specimens with galvanized reinforcement exhibited less staining than those with conventional reinforcement, especially for specimens with 2 in. (51 mm) cover, as shown in Fig. 4(a) and 4(b).

An autopsy of the specimens with conventional reinforcement showed heavy corrosion losses over the entire bar surface (Fig. 5(a)). The galvanized reinforcement exhibited heavy corrosion losses over most of the bar surface, but with some sections exhibiting little to no loss in zinc (Fig. 5(b)). Most of the uncorroded regions were located on the top face of the bar, which is likely the result of the bottom side of the bar having more uniform exposure to the ions migrating from the bottom bars, as would be expected in impressed current specimens. For the galvanized bars with 1 or 2 in. (25.4 or 51 mm) cover, corrosion occurred over approximately 90% of the total surface area; for bars with 0.5 in. (12.7 mm) cover, the corroded area was approximately 70% of the total surface area. Correcting for the area exhibiting corrosion would increase the apparent depth of corrosion loss on the galvanized bars. For example, the average corrosion loss to cause cracking on the galvanized bars with 1 in. (25.4 mm) cover would increase from 1.96 mils to 2.18 mils (49.8 μm to 55.4 μm). The corrosion products in the concrete surrounding the galvanized reinforcement resembled

those seen in specimens with conventional reinforcement, suggesting that the bulk of the corrosion products applying pressure to the surrounding concrete were corrosion products of iron and not those of zinc.

To determine if the corrosion of the steel observed on the galvanized reinforcement was also present at crack initiation, two additional specimens with galvanized reinforcement and 1 in. (25.4 mm) cover were cast and autopsied at the onset of cracking. The autopsy revealed the presence of localized steel corrosion, with corrosion products similar to those observed on the specimens autopsied after the crack had propagated and widened, suggesting that the observed cracks were not due to the buildup of zinc corrosion prod-

(a)

(b)

Fig. 4—Concrete surface at end of testing: (a) conventional reinforcement, impressed current, 2 in. (25.4 mm) cover; and (b) galvanized reinforcement, impressed current, 2 in. (25.4 mm) cover.

ucts, but possibly due to the formation of corrosion products from the intermetallic iron-zinc layers or from the underlying steel. A chemical analysis of the corrosion products was beyond the scope of this study, but the telltale orange-brown ferric oxide corrosion products strongly suggest corrosion of underlying steel.
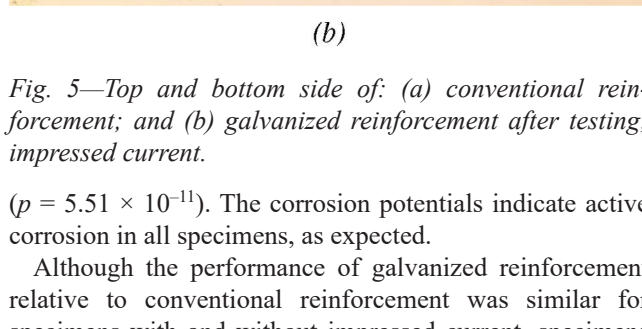
Specimens without impressed current

Specimens without impressed current were only tested until a crack initiated. All cracks initiated in the center third of the beam, as observed in the impressed current specimens. The corrosion loss at crack initiation (as measured by linear polarization resistance) and age at crack initiation for conventional and galvanized reinforcement are shown in Table 5. Corrosion potentials with respect to a copper/copper sulfate electrode (CSE) for conventional and galvanized reinforcement are shown in Fig. 6(a) and 6(b), respectively. Based on the total area of the bars, the specimens with galvanized reinforcement cracked at an average corrosion loss of 0.489 mils (12.4 μm), which is over twice the average corrosion loss required to crack concrete with conventional reinforcement (0.213 mils [5.41 μm]). The ratio is similar to that observed for the specimens with impressed current. The time to crack initiation was almost four times longer for galvanized reinforcement (81 weeks) than for conventional reinforcement (21 weeks). Based on Student's t-test, the difference in performance between conventional and galvanized reinforcement was statistically significant for both corrosion loss at crack initiation ($p = 1.67 \times 10^{-5}$) and time to cracking
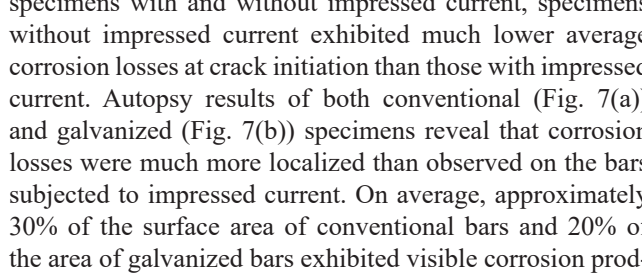

(a)
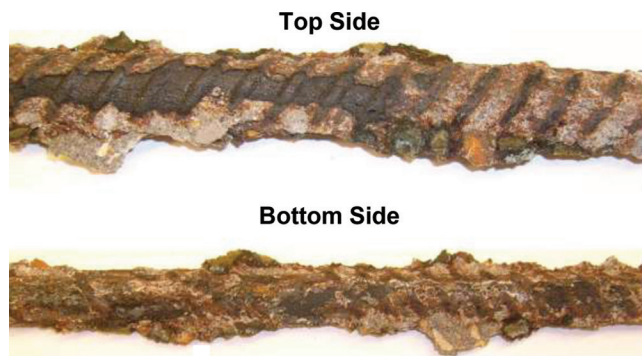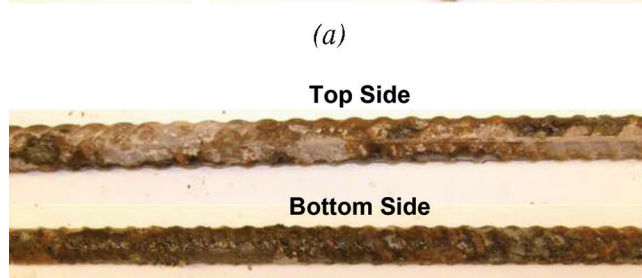
(b)

Fig. 5—Top and bottom side of: (a) conventional reinforcement; and (b) galvanized reinforcement after testing; impressed current.

($p = 5.51 \times 10^{-11}$). The corrosion potentials indicate active corrosion in all specimens, as expected.

Although the performance of galvanized reinforcement relative to conventional reinforcement was similar for specimens with and without impressed current, specimens without impressed current exhibited much lower average corrosion losses at crack initiation than those with impressed current. Autopsy results of both conventional (Fig. 7(a)) and galvanized (Fig. 7(b)) specimens reveal that corrosion losses were much more localized than observed on the bars subjected to impressed current. On average, approximately 30% of the surface area of conventional bars and 20% of the area of galvanized bars exhibited visible corrosion products, compared to 100% and 90%, respectively, for the specimens with an impressed current. When correcting for the area of the bar exhibiting active corrosion, corrosion losses at cracking of 0.71 and 2.07 mils (18.0 and 52.6 μm) were observed for conventional and galvanized reinforcement, respectively, which are comparable to the values of 0.88 and 2.18 mils (22.4 and 55.4 μm) based on the area of the bars exhibiting active corrosion observed for the impressed current specimens with 1 in. (25.4 mm) cover.

DISCUSSION

Across all tests, galvanized reinforcement required greater losses to cause cracking of the concrete than conventional reinforcement. Furthermore, autopsies of specimens with galvanized reinforcement revealed corrosion products of iron and a localized loss of the zinc layer. Given that the galvanized reinforcement exhibited greater losses at cracking, this suggests that the corrosion products of zinc subject to chloride-induced corrosion are not as expansive as those of iron. This behavior was observed both with and without the use of an impressed current. A visual observation

Table 5—Corrosion losses at crack initiation for conventional and galvanized reinforcement for specimens without impressed current, mils (1 in. [25.4 mm] cover)

Specimen	Conventional			Galvanized		
	Cracking age, weeks	Corrosion loss*	Corrosion loss†	Cracking age, weeks	Corrosion loss*	Corrosion loss†
1	16	0.175	0.583	84	0.512	2.56
2	21	0.240	0.800	78	0.434	2.17
3	19	0.161	0.537	85	0.632	3.16
4	27	0.264	0.880	82	0.473	2.37
5	22	0.231	0.770	77	0.476	2.38
6	22	0.204	0.680	78	0.408	2.04
Average	21.2	0.213	0.710	80.7	0.489	2.45
Std. dev.	3.7	0.040	0.132	3.4	0.079	0.394

*Assuming entire area of bar is undergoing active corrosion.

†Based on percentage of bar surface area exhibiting active corrosion (30% for conventional bars, 20% for galvanized bars).

Notes: 1 mil = 25.4 μm = 0.0254 mm; 1 in. = 25.4 mm.
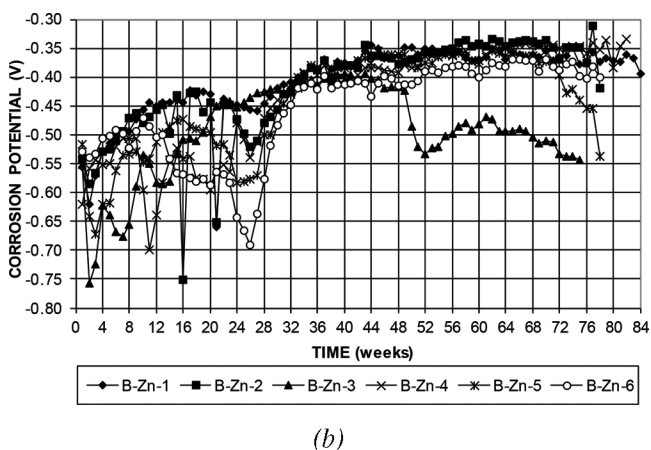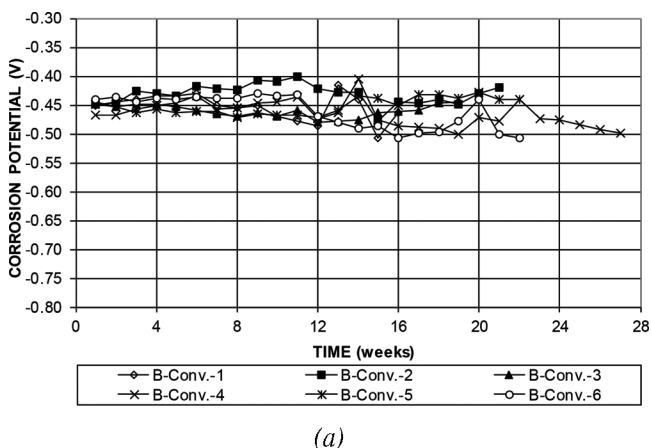

(a)

(b)

Fig. 6—Top bar corrosion potential versus time for specimens with: (a) conventional reinforcement; and (b) galvanized reinforcement; no impressed current.

(a)

(b)

Fig. 7—Top and bottom side of: (a) conventional reinforcement; and (b) galvanized reinforcement after testing; no impressed current.

of corrosion products on the bars and on the surface of the concrete suggests that corroding galvanized reinforcement will not result in spalling of the concrete until the underlying intermetallic layers or steel is corroding; further research is needed to quantify this finding, however.

The similarity in results for specimens with and without impressed current, when adjusted for corroded area, provide a strong indication that loc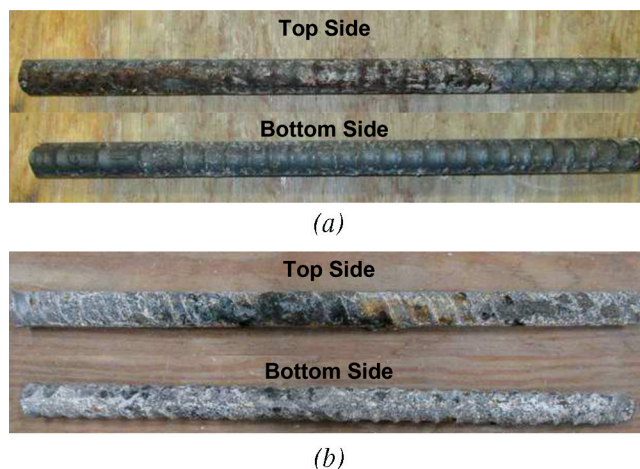al corrosion losses control cracking and that corrosion losses of similar magnitude (expressed in depth of loss), whether over the full bar surface or over smaller regions spaced along a bar, will have the same effect on cracking. The results also show that for uncoated reinforcement, impressed current may be used to establish the corrosion loss required to cause cracking and calibrate expressions connecting crack initiation with member geometry, but that to be useful for practical application, the results need to be interpreted in terms of both the total corrosion loss and the distribution of that loss in structures.

Although beyond the scope of this study, establishing the constituents of the zinc and iron corrosion products may be of interest, especially in light of the mixed performance of galvanized reinforcement observed by previous researchers.

SUMMARY AND CONCLUSIONS

The research presented in this paper examines the corrosion losses on conventional and galvanized reinforcement required to crack concrete. Specimens had concrete covers ranging from 0.5 to 2 in. (12.7 to 51 mm) to establish a relationship between corrosion loss and cracking. The following conclusions are based on the data and analyses presented in this report.

1. For the combinations of reinforcement and concrete cover tested, galvanized reinforcement required over twice the corrosion loss to crack concrete as conventional reinforcement.

2. Cracking due to corrosion of galvanized reinforcement appears to involve the buildup of corrosion products from the underlying intermetallic layers or from the underlying steel.

3. The use of impressed current did not appreciably alter the relative performance of the bars. Differences in corrosion patterns and total material loss were observed compared to specimens without an impressed current, but when adjusted for corroded area, the magnitudes of corrosion loss required to crack concrete are similar for bars with and without impressed current.

4. Local, rather than average, corrosion losses control cracking of concrete adjacent to galvanized reinforcement.

AUTHOR BIOS

ACI member **Matthew O'Reilly** is an Assistant Professor of Civil, Environmental, and Architectural Engineering at the University of Kansas, Lawrence, KS. He received his BS in mechanical engineering from the University of Rochester, Rochester, NY, and his MS and PhD in civil engineering from the University of Kansas. He is a member of ACI Committees 123, Research and Current Developments; and 222, Corrosion of Metals in Concrete.

ACI member **Omid Farshadfar** is a Project Engineer with Thornton Tomasetti, Kansas City, MO. He received his BS and MS in civil and structural engineering, respectively, from Isfahan University of Technology, Isfahan, Iran, and his PhD in civil engineering from the University of Kansas.

ACI Honorary Member **David Darwin** is the Deane E. Ackers Distinguished Professor and Chair of the Department of Civil, Environmental, and Architectural Engineering at the University of Kansas and a Past President of ACI. He is a member of ACI Committees 222, Corrosion of Metals in Concrete; 224, Cracking; ACI Subcommittee 318-B, Anchorage and Reinforcement (Structural Concrete Building Code); and Joint ACI-ASCE Committees 408, Bond and Development of Steel Reinforcement; 445, Shear and Torsion; and 446, Fracture Mechanics of Concrete.

JoAnn Browning, FACI, is the Dean of the School of Engineering and the David and Jennifer Spencer Distinguished Chair at the University of Texas at San Antonio, San Antonio, TX. She is a member of the ACI Board of Direction and the ACI Technical Activities Committee, as well as a member of ACI Committees 314, Simplified Design of Concrete Buildings; 318, Structural Concrete Building Code; 341, Earthquake-Resistant Concrete Bridges; 374, Performance-Based Seismic Design of Concrete Buildings; and Joint ACI-ASCE Committee 408, Bond and Development of Steel Reinforcement.

Carl E. Locke Jr. is Professor Emeritus of chemical and petroleum engineering and former Dean of Engineering at the University of Kansas. His research interests include corrosion of steel in concrete.

REFERENCES

Abouhussien, A., and Hassan, A., 2016, "Cover Crack Growth Monitoring in RC Structures Subjected to Corrosion with Acoustic Emission Sensors," Resilient Infrastructure: CSCE Annual Conference, June, 10 pp.

Alonso, C.; Andrade, C.; Rodriguez, J.; and Diez, J. M., 1998, "Factors Controlling Cracking of Concrete Affected by Reinforcement Corrosion," Materials and Structures, V. 31, No. 7, Aug.-Sept., pp. 435-441. doi: 10.1007/BF02480466

Andrade, M. C., and Macias, A., 1988, "Galvanized Reinforcements in Concrete," Surface Coatings-2, A. D. Wilson, J. W. Nicolson, and H. J. Prosser, eds., Elsevier Applied Science, London, UK, pp. 137-182.

ASTM A615/A615M, 2009, "Standard Specification for Deformed and Plain Carbon Steel Bars for Concrete Reinforcement," ASTM International, West Conshohocken, PA, 6 pp.

ASTM A767/A767M, 2009, "Standard Specification Zinc-Coated (Galvanized) Steel Bars for Concrete Reinforcement," ASTM International, West Conshohocken, PA, 5 pp.

Belaïd, F.; Arliguie, G.; and François, R., 2001, "Porous Structure of the ITZ around Galvanized and Ordinary Steel Reinforcements," Cement and Concrete Research, V. 31, No. 11, Nov., pp. 1561-1566. doi: 10.1016/S0008-8846(01)00597-X

Darwin, D.; Browning, J.; Lindquist, W.; McLeod, H. A. K.; Yuan, J.; Toledo, M.; and Reynolds, D., 2010, "Low-Cracking, High-Performance Concrete Bridge Decks—Case Studies Over the First 6 Years," Transportation Research Record: Journal of the Transportation Research Board, V. 2202, No. 1, pp. 61-69. doi: 10.3141/2202-08

Darwin, D.; Browning, J.; O'Reilly, M.; Locke, C. E.; and Virmani, Y. P., 2011, "Multiple Corrosion-Protection Systems for Reinforced Concrete Bridge Components," Publication No. FHWA-HRT-11-060, Federal Highway Administration, Washington, DC, Aug. 2011, 256 pp.

Darwin, D.; Browning, J.; O'Reilly, M.; Xing, L.; and Ji, J., 2009, "Critical Chloride Corrosion Threshold of Galvanized Reinforcing Bars," ACI Materials Journal, V. 106, No. 2, Mar.-Apr., pp. 176-183.

El Maaddawy, T., and Soudki, K., 2003, "Effectiveness of Impressed Current Technique to Simulate Corrosion of Steel Reinforcement in Concrete," Journal of Materials in Civil Engineering, ASCE, V. 15, No. 1, Jan.-Feb., pp. 41-47. doi: 10.1061/(ASCE)0899-1561(2003)15:1(41)

Farshadfar, O.; O'Reilly, M.; and Darwin, D., 2017, "Performance Evaluation of Corrosion Protection Systems for Reinforced Concrete," SM Report No. 122, University of Kansas Center for Research, Lawrence, KS, Jan., 378 pp.

Hime, W., and Machin, M., 1993, "Performance Variations of Galvanized Steel in Mortar and Concrete," Corrosion, V. 49, No. 10, Oct., pp. 858-860. doi: 10.5006/1.3316010

Nossoni, A., and Harichandran, R., 2014, "Electrochemical-Mechanistic Model for Concrete Cover Cracking Due to Corrosion Initiated by Chloride Diffusion," Journal of Materials in Civil Engineering, ASCE, V. 26, No. 6, June, pp. 1-10. doi: 10.1061/(ASCE)MT.1943-5533.0000470

O'Reilly, M.; Darwin, D.; Browning, J.; and Locke, C., 2011, "Evaluation of Multiple Corrosion Protection Systems for Reinforced Concrete Bridge Decks," SM Report No. 100, University of Kansas Center for Research, Lawrence, KS, Jan., 535 pp.

Rasheeduzzafar; Al-Saadoun, S. S.; and Al-Gahtani, A., 1992a, "Corrosion Cracking in Relation to Bar Diameter, Cover, and Concrete Quality," Journal of Materials in Civil Engineering, ASCE, V. 4, No. 4, Nov., pp. 327-342.

Rasheeduzzafar; Dakhil, F. H.; Bader, M. A.; and Khan, M. K., 1992b, "Performance of Corrosion Resisting Steels in Chloride-Bearing Concrete," ACI Materials Journal, V. 89, No. 5, Sept.-Oct., pp. 439-448.

Sergi, G.; Short, N.; and Page, C., 1985, "Corrosion of Galvanized and Galvanannealed Steel in Solutions of pH 9.0-14.0," Corrosion/85, Boston, MA, Mar. 25-29.

Suda, K.; Misra, S.; and Motohashi, K., 1993, "Corrosion Products of Reinforcing Bars Embedded in Concrete," Corrosion Science, V. 35, No. 5-8, July, pp. 1543-1549. doi: 10.1016/0010-938X(93)90382-Q

Tittarelli, F.; Moriconi, G.; Gasparri, G.; and Fratesi, R., 2000, "Comparative Evaluation of Traditional and Innovative Corrosion Protection Methods in Cracked Reinforced Concrete Exposed to Chloride Environment," Durability of Concrete, Proceedings of the Fifth International ACI/CANMET Conference, SP-192, V. M. Malhotra, ed., American Concrete Institute, Farmington Hills, MI, pp. 613-628.

Torres-Acosta, A., and Sagues, A., 2004, "Concrete Cracking by Localized Steel Corrosion-Geometric Effects," ACI Materials Journal, V. 101, No. 6, Nov.-Dec., pp. 501-507.

Williamson, G., 2007, "Service Life Modeling of Virginia Bridge Decks," PhD thesis, Department of Civil and Environmental Engineering, Virginia Polytechnic Institute and State University, Blacksburg, VA, 210 pp.

Williamson, G.; Weyers, R.; Sprinkel, M.; and Brown, M., 2009, "Concrete and Steel Type Influence on Probabilistic Corrosion Service Life," ACI Materials Journal, V. 106, No. 1, Jan.-Feb., pp. 82-88.

Xia, J., and Jin, W., 2014, "Prediction of Corrosion-Induced Crack Width of Corroded Reinforced Concrete Structures," Proceedings of the 4th International Conference on the Durability of Concrete Structures, ICDCS 2014, July, pp. 46-54.

Yeomans, S., 1994, "A Conceptual Model for the Corrosion of Galvanized Steel Reinforcement in Concrete," Corrosion and Corrosion Protection, University of Sheffield, Sheffield, UK, pp. 1299-1309.

Zhao, Y.; Yu, J.; and Jin, W., 2011, "Damage Analysis and Cracking Model of Reinforced Concrete Structures with Rebar Corrosion," Corrosion Science, V. 53, No. 10, Oct., pp. 3388-3397. doi: 10.1016/j.corsci.2011.06.018